Carbohydrate Polymers 98 (2013) 412–420

Contents lists available at SciVerse ScienceDirect

Carbohydrate Polymers

journal homepage: www.elsevier.com/locate/carbpol

Dissolution of cellulose from AFEX-pretreated *Zoysia japonica* in AMIMCl with ultrasonic vibration

Le Liu, Meiting Ju*, Weizun Li, Qidong Hou

College of Environmental Science and Engineering, Nankai University, Tianjin 300071, PR China

ARTICLE INFO

Article history:
Received 26 March 2013
Received in revised form 13 May 2013
Accepted 18 June 2013
Available online 27 June 2013

Keywords:
1-Allyl-3-alkylimidazolium chloride ionic liquid
AFEX
Dissolution
Ultrasonic vibration
Regenerated cellulose

ABSTRACT

In this study, 1-allyl-3-methylimidazolium chloride (AMIMCl), an ionic liquid, was synthesized and characterized by a series of test methods. Pretreatment of *Zoysia japonica* by ammonia fiber expansion (AFEX) was shown to reduce significantly the mass of hemicellulose and lignin in biomass, thereby breaking the lignocellulosic structure. *Z. japonica* samples pretreated with AFEX showed reasonable solubility in AMIMCl upon ultrasonic treatment. The rate of cellulose regeneration from *Z. japonica* samples pretreated with AFEX increased with increase in applied power of ultrasonication within a certain power range from 0 to 110 W. The regeneration rate of cellulose from AFEX-pretreated *Z. japonica* reached a maximum of 97% when the ultrasonic power was 110 W. Fourier transform infrared spectroscopy and nuclear magnetic resonance analyses indicated that the regenerated cellulose was similar to microcrystalline cellulose.

1. Introduction

In China, the "National Long-Term Science and Technology Development Plan (2006–2020)" points out that agricultural biomass is one of the key development areas. Plants, which produce 100 billion tons of cellulose through photosynthesis annually (Zhu et al., 2006), are regarded as an inexhaustible, renewable resource. Plant-derived cellulose is widely used in the textile, chemical, pharmaceutical, and energy industries because it does not contribute to pollution and is biocompatible, biodegradable, and abundant (Zhang, Lv, & Luo, 2011). Moreover, agricultural solid wastes can be used as important lignocellulosic feedstock (Heinze & Liebert, 2001; Zhu et al., 2006). Although the biochemical conversion of biomass into energy and industrial raw materials has significant technical and economic potential, lignocellulosic biomass is naturally resistant to chemical degradation. This resistance is due to various physical and chemical factors, such as the presence of lignin, the crystallinity of cellulose, and the presence of covalent cross-linkages between lignin and hemicelluloses in the plant cell wall (Li et al., 2010). Cellulose is a linear homopolymer of β(1 → 4)-linked D-glucopyranose units that may aggregate to form a highly ordered structure. The chemical constitution and spatial conformation of cellulose account for its aggregation tendencies (Klemm, Philipp, Heinze, Heinze, & Wagenknecht, 1998; Oh et al., 2005).

Various pretreatment techniques may be used to enhance the breakdown of lignocellulosic biomass. Some of the most popular techniques are fermentative processes, which include ammonia fiber expansion (AFEX). AFEX offers several advantages: It reduces the production of inhibitory compounds and it precludes the washing step in removing inhibitors and pretreatment catalyst. It also requires minimal nutrients supplied to the fermentation organisms because the process leaves traces of residual ammonia and native plant-derived micronutrients in the recovered pretreatment product (Chundawat et al., 2011, 2010). In a typical AFEX process, aqueous ammonia is added to the biomass and the resulting mixture is heated to moderate temperatures (70–100 °C) and pressures (150–400 psi). After 5 to 30 min, the pressure is quickly released. About 99% of the ammonia can be recovered in the gas phase and recycled. AFEX results in partial solubilization of hemicelluloses (Chundawat et al., 2010; Mosier et al., 2005). The process apparently causes the movement of solubilized hemicelluloses and migration of lignin components to the exterior surface of the cell walls, which increases enzyme accessibility to the cell wall polysaccharides (Chundawat et al., 2010; Kim et al., 2008).

The development of a new type of cellulose solvent would make a significant contribution to the sustainable and efficient use of cellulose resources in agricultural solid waste. Several suitable solvent systems for dissolving cellulose have been reported, e.g., *N*-methylmorpholine-*N*-oxide (Doganand & Hilmioglu, 2009), LiCl/N, *N*-dimethylacetamide (DMAc) (Nattakan, Takashi, &, Ton, 2009),

* Corresponding author at: College of Environmental Science and Engineering, Nankai University, 94 Weijin Street, Tianjin 300071, PR China. Tel.: +86 13820988813; fax: +86 2223506446.
E-mail address: jumeit@nankai.edu.cn (M. Ju).

0144-8617/$ – see front matter © 2013 Elsevier Ltd. All rights reserved.
http://dx.doi.org/10.1016/j.carbpol.2013.06.030

and NaOH/urea (Song, Zhang, Gan, Zhou, &, Zhang, 2010). Although they can readily dissolve cellulose, their disadvantages, such as high cost, recovery difficulties, and toxicity, limit their use (Liu & Zhang, 2009).

Ionic liquids, also known as low-temperature molten salts or designable solvents, have been recognized to comprise a new kind of green solvent (Deng, 2003). They offer various advantages that allow them to be widely used in chemical synthesis, extraction and separation, materials preparation, and other fields. Ionic liquids consist solely of cations and anions that are present in liquid form at or near room temperature. Ionic liquids have unique physical and chemical properties, such as low melting point (up to 173 K), higher solubility, and designable selective dissolution.

In 2002, Rogers et al. first reported the solubility of natural cellulose in a series of ionic liquids such as 1-butyl-3-methylimidazolium chloride (BMIMCl) (Swatloski, Spear, Holbrey, &, Rogers, 2002). BMIMCl is a nonvolatile, strong solvent for cellulose and is easily recovered after processing. These attributes prompted further research on the regulation and design of cation–anion structures to obtain new types of ionic liquids with superior properties. In 2003, Ren et al. introduced the allyl group to the cationic structure of an ionic liquid to prepare 1-allyl-3-methylimidazolium chloride (AMIMCl), which has excellent solvent properties (Ren, Wu, Zhang, He, &, Guo, 2003).

In the present study, AMIMCl was synthesized from *N*-methylimidazole and allyl chloride and was characterized by a series of test methods. Cellulose from *Zoysia japonica* samples was pretreated by AFEX (these treated samples are hereafter known as ZJ-AFEX). We focused on the dissolution of ZJ-AFEX in AMIMCl upon ultrasonic treatment. The regenerated cellulose was characterized by Fourier transform infrared (FTIR) spectroscopy and nuclear magnetic resonance (NMR) analyses. This paper provides the necessary theoretical basis for the development of ionic liquids for utilization of biomass feedstock resources.

2. Materials and methods

2.1. Materials

Samples of *Z. japonica* were collected from agricultural fields in Tianjin in northern China. After drying at 60 °C in an oven for 16 h, the grass samples were ground to particles that pass through a 0.7 mm screen. The fiber components of *Z. japonica* were analyzed according to the Van Soest method, using a FOSS Fibertec 2010 fully automated fiber analysis system. This determination revealed the following composition: lignin, 19.87% (w/w); hemicellulose, 40.86% (w/w); cellulose, 29.71% (w/w). Microcrystalline cellulose was purchased from Serva (Heidelberg, Germany). *N*-Methylimidazole was purchased from Tianjin Xuanyang Industrial Co., Ltd. (Tianjin, China), and purified by reduced-pressure distillation before synthesis. Allyl chloride (analytical reagent grade; 98% pure) with a specific gravity of 0.935 kg/m^3 was purchased from Shanghai Kefeng (Shanghai) Trading Co., Ltd., Shanghai, China.

2.2. AFEX pretreatment of Z. japonica

A measured amount of *Z. japonica* was dispersed in water by magnetic stirring for 24 h and then diluted to 5% (w/w). Subsequently, the pre-wetted *Z. japonica* was loaded into the AFEX reactor. The ratio of anhydrous ammonia to *Z. japonica* ranged from 0.5:1 to 2:1, and the reaction was carried out at 120 °C and 200 psi for 30 min. This process yielded ZJ-AFEX. The lignocellulose residual rate and mass loss rate of *Z. japonica* after AFEX pretreatment were calculated according to Eqs. (1) and (2):

$$R_{s,i} = \frac{M_{r,i}}{M_{o,i}} \quad (1)$$

$$R_l = 1 - \frac{M_{rZJ}}{M_{oZJ}} \quad (2)$$

where i represents cellulose, hemicellulose, and lignin; $R_{s,i}$ is the residual rate; $M_{r,i}$ is the mass of the residual cellulose, hemicellulose, or lignin in the *Z. japonica* sample after AFEX pretreatment; $M_{o,i}$ is the mass of cellulose, hemicellulose, or lignin in the original *Z. japonica* sample; R_l is the mass loss rate; M_{rZJ} is the mass of the residual *Z. japonica* sample after AFEX pretreatment; M_{oZJ} is the mass of the original *Z. japonica* sample.

2.3. Synthesis and characterization of AMIMCl

The general synthesis of AMIMCl was performed according to the method described in a previous report (Ren et al., 2003). Allyl chloride was added dropwise to *N*-methylimidazole under an argon atmosphere to the final allyl chloride/*N*-methylimidazole molar ratio of approximately 1:1.2. The entire reaction was carried out in a 500 mL glass-lined reactor at room temperature. When all of the allyl chloride was added, the reaction mixture was refluxed with magnetic stirring at 55 °C for about 10 h. After removing the residual allyl chloride under reduced pressure, the resulting liquid was repeatedly washed with an excess amount of ether to eliminate the residual *N*-methylimidazole. The resulting ionic liquid, AMIMCl, was dried at 80 °C for 72 h. The purity of the AMIMCl was determined by ^{1}H NMR spectroscopy.

2.4. Dissolution of cellulose

The dissolution of *Z. japonica* and ZJ-AFEX samples in AMIMCl under an argon atmosphere were investigated. For the dissolution process, 2.00 g of sample was added to 50.00 g of ionic liquid. The mixture was placed in a KQ3200DE ultrasonic oscillator (set at a specific power) at 80 °C for 30 min. The remaining insoluble residue was filtered under vacuum using a 60 mL G3 sand-core bush funnel, and then dried at 105 °C for 3 h. The resulting filtrate containing the cellulose was collected to regenerate the cellulose. The solubility of the sample in AMIMCl was calculated as shown in Eq. (3):

$$R_d = 1 - \frac{M_r}{M_o} \quad (3)$$

where R_d is the solubility in AMIMCl; M_r is the mass of the residual sample after dissolution in AMIMCl; M_o is the mass of the original sample.

2.5. Preparation of the regenerated cellulose

After dissolution of the sample in AMIMCl, the resulting filtrate containing cellulose was combined with an excess amount of deionized water to regenerate the cellulose. The regenerated cellulose samples were dried at 80 °C for 72 h. The cellulose regeneration rate was calculated as shown in Eq. (4):

$$R_r = 1 - \frac{M_{r-cel}}{M_{o-cel}} \quad (4)$$

where R_r is the cellulose regeneration rate; M_{r-cel} is the mass of residual cellulose in the sample after dissolution in AMIMCl; M_{o-cel} is the mass of cellulose in the original sample.

2.6. Recycling of AMIMCl

After sample dissolution and cellulose extraction, recovery of the AMIMCl was accomplished by evaporating water from the

filtrate. The recycled AMIMCl was used to extract cellulose, as described in Sections 2.4 and 2.5.

2.7. Characterization

2.7.1. FTIR

All samples were ground into a powder and vacuum-dried for 24 h. The IR spectra of the samples were recorded using an FTS6000 Fourier Transform IR spectrometer (Bio-rad, USA). Test specimens were prepared according to the KBr disk method.

2.7.2. Polarization microscopy (POM)

The regenerated cellulose from ZJ-AFEX was mounted onto a metal-base specimen holder using double-sided sticky tape. The sample was then coated with the synthesized AMIMCl using a vacuum sputter-coater. Afterward, the sample structures were observed continuously at 80 °C for 60 min using a Linkam THMSE600-BX51 polarized optical microscope (Olympus, Japan) equipped with a hot stage and a digital camera.

2.7.3. NMR

Solid-state cross-polarization/magic angle spinning ^{13}C NMR spectra of the regenerated cellulose were obtained using a Bruker Infinityplus-400 NMR spectrometer. The instrument was equipped with a 4 mm MAS probe and was operated at a frequency of 100.37 MHz. The structure of AMIMCl in D_2O at room temperature was determined by ^{1}H NMR spectroscopy. Analysis was carried out on a Mercury Vx-300 with a 5 mm BBO probe at a frequency of 100.61 MHz.

2.7.4. Thermogravimetric analysis (TGA)

The thermal stability of AMIMCl was investigated using a TG209 TGA instrument (NETZSCH, Ltd., Germany). Weight loss was recorded in the range of 0–550 °C, and the sample was heated at a rate of 10 °C/min.

2.7.5. Scanning electron microscopy (SEM) analysis

The original *Z. japonica* and ZJ-AFEX samples, obtained by air drying method, were fixed to a metal-base specimen holder using double-sided sticky tape. The samples were then coated with gold using a vacuum sputter-coater. Afterwards, the fracture surfaces were observed using an S-3700N scanning electron microscope (Hitachi, Ltd., Japan).

3. Results and discussion

3.1. Characteristics of AMIMCl

The process developed in the current study (Wu et al., 2004; Zhang, Wu, Zhang, &, He, 2005) was successfully used to synthesize AMIMCl. The AMIMCl exhibited a considerable capacity to dissolve cellulose in *Z. japonica*, as observed by polarization microscopy. Fig. 1A and B show that dissolution of the cellulose samples commenced because of the dispersion of numerous cellulose fibers in

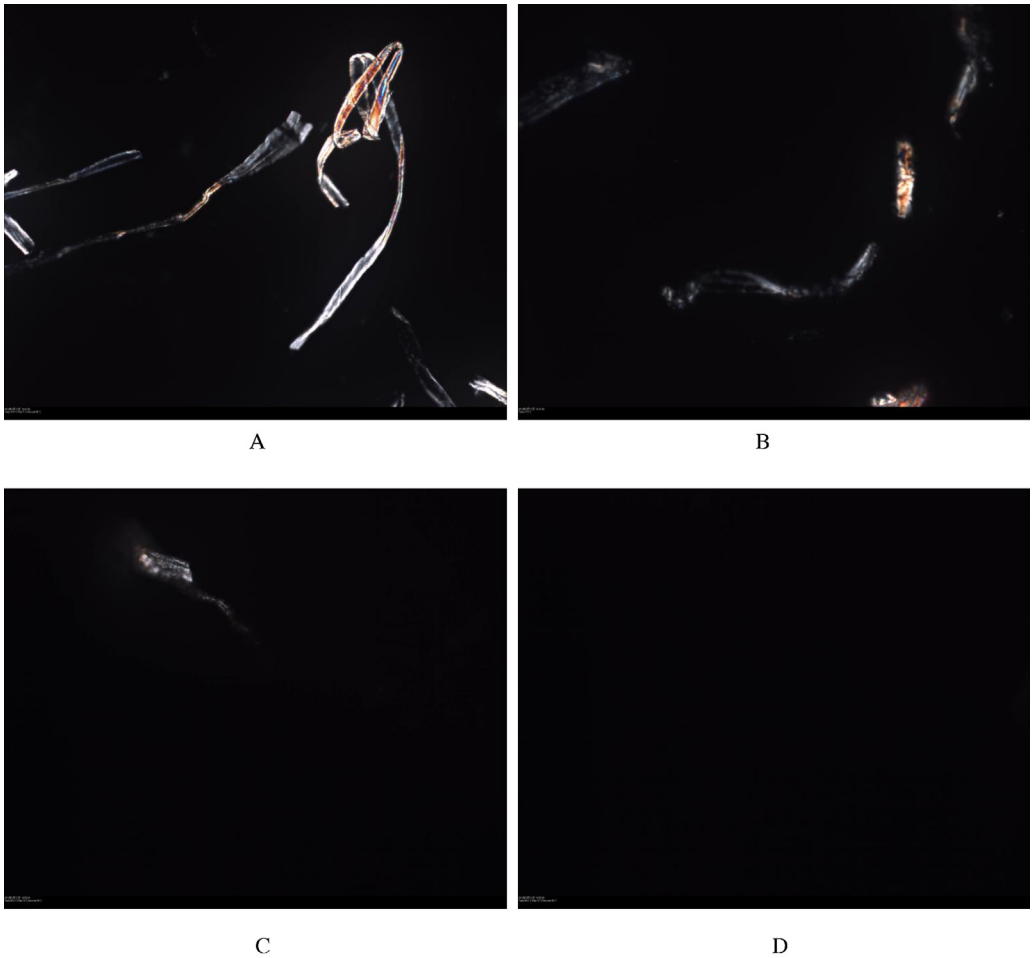

Fig. 1. Dissolution of cellulose in *Zoysia japonica* in AMIMCl in the initial stage (A), partially dissolved stage (B), later dissolved stage (C) completely dissolved stage, and (D) the micrographs were magnified two hundred times.

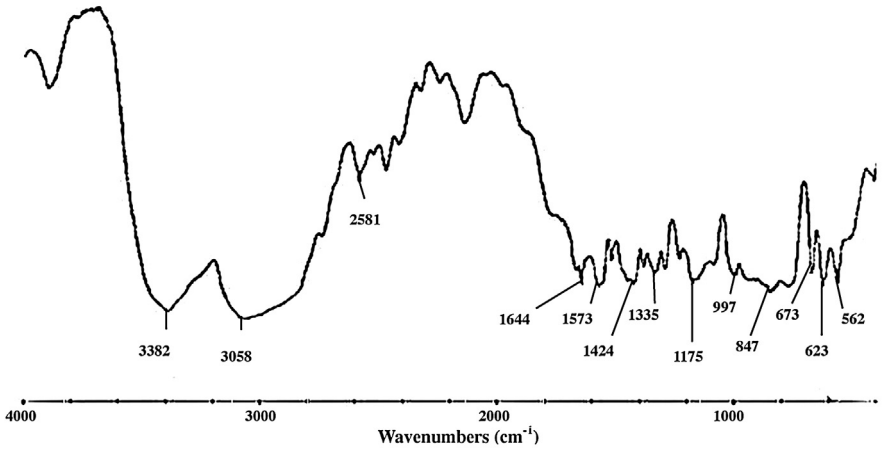

A

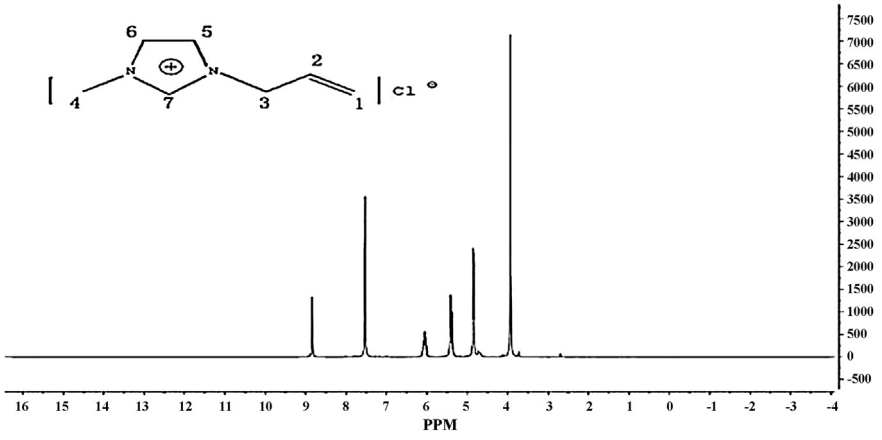

B

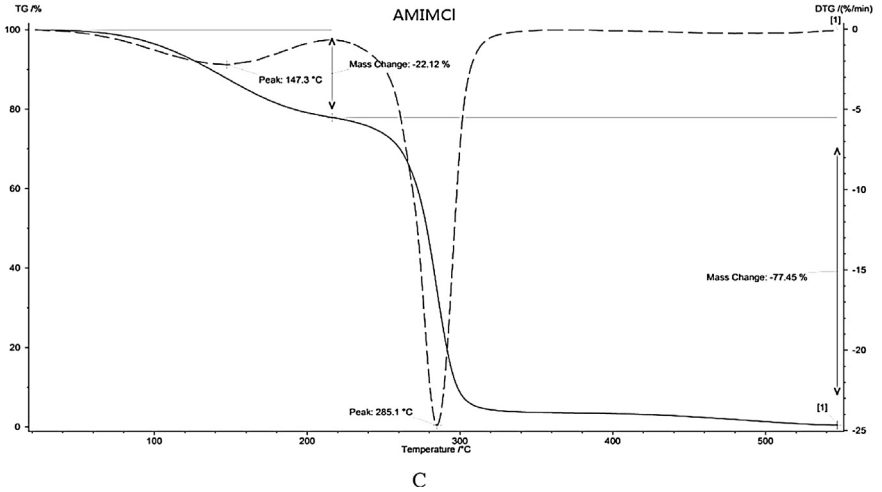

C

Fig. 2. FT-IR spectrum of AMIMCl (A), ^{1}H NMR spectrum of AMIMCl (B) and TGA/DTG curve of AMIMCl (C).

the ionic liquid. Eventually, the cellulose fibers disintegrated and disappeared, while a blackburst structure emerged, as shown in the polarization micrographs (Fig. 1D).

The FTIR spectrum of AMIMCl (Fig. 2A) shows the peaks at the following wavenumbers (in cm^{-1}): 3058 (C═C—H stretching vibration), 1644 (C═C stretching vibration in allyl), 1573 (C═N stretching vibration in imidazole ring), 1424 (—CH_2/C—H bending vibration in side chain), 1335 (C—N stretching vibration), 1175 (C—H bending vibration in imidazole ring), and 997 (C—H rocking vibration in allyl). The peak at 3382 cm^{-1} corresponds to trace water accumulated due to the hygroscopicity of AMIMCl. The FTIR spectrum of the regenerated AMIMCl is similar to the

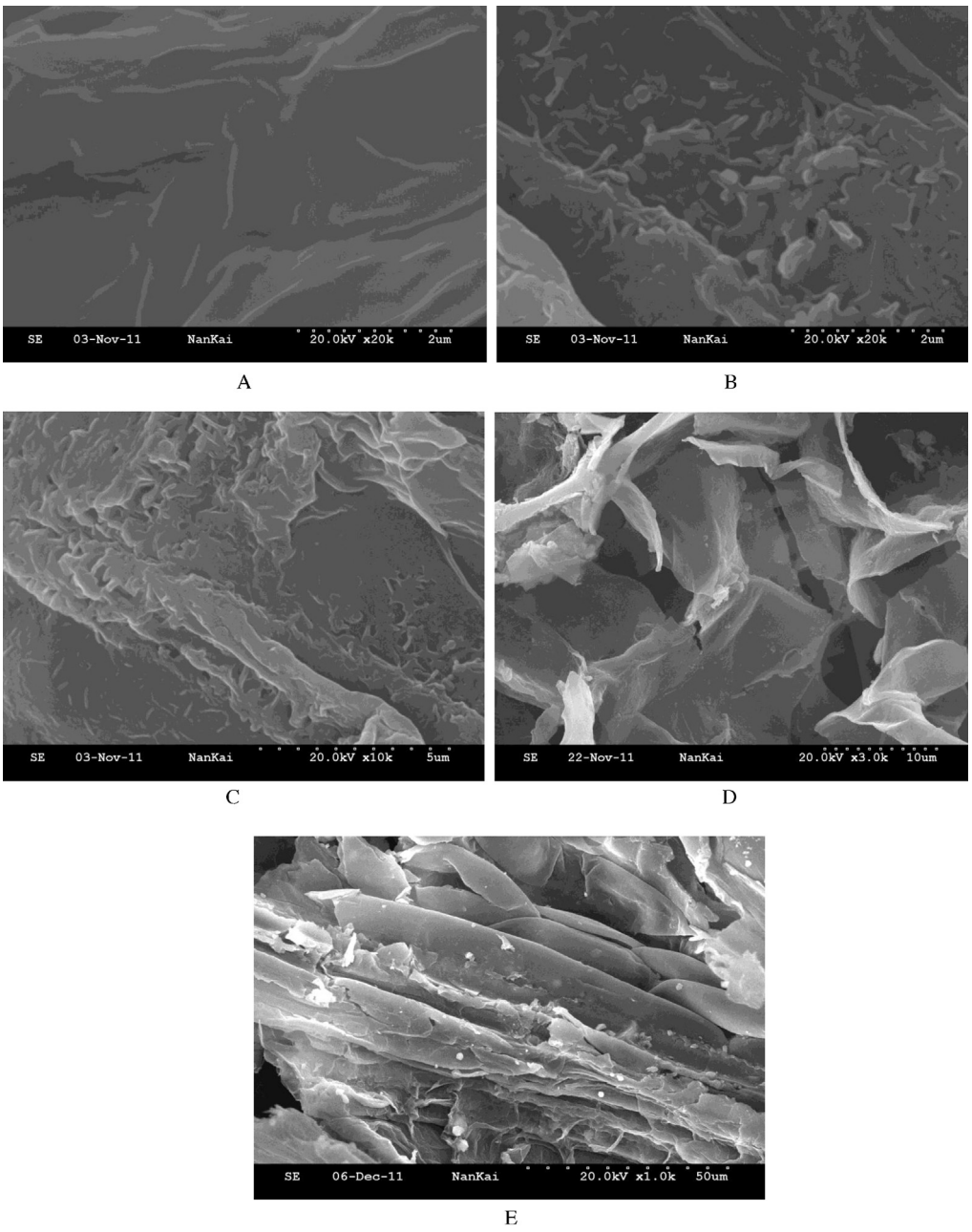

Fig. 3. Structures of original *Zoysia japonica* (A), *Z. japonica* sample after AFEX pretreatment with a ratio of anhydrous ammonia to *Z. japonica* 0.5:1 (B), ratio 1:1 (C), ratio 1.5:1 (D), and ratio 2:1 (E).

spectrum of the as-synthesized AMIMCl, and shows the same peaks.

The ^{1}H NMR spectrum of AMIMCl (Fig. 2B) shows the peaks corresponding to the following chemical shifts (in ppm): $\delta = 4.85$, $\delta = 5.56$, $\delta = 6.05$, $\delta = 3.93$, and $\delta = 8.87$. These shifts are related to hydrogen atoms 1, 2, 3, 4, and 7, respectively. The peak at $\delta = 7.53$ is related to hydrogen atoms 5 and 6. The peaks in the ^{1}H NMR spectrum of the regenerated AMIMCl are similar to those in this spectrum except for the peak at $\delta = 3.41$, which corresponds to the signal for trace water.

The TGA curve for AMIMCl is shown in Fig. 2C. In the thermal degradation process, the ionic liquid was stable below 200 °C. The weight loss (nearly 20%) below 200 °C was caused by the evaporation of water and traces of remaining reactant. The decomposition temperature corresponding to the maximum rate of weight loss (T_d) was 285.1 °C, and the corresponding weight loss between 200 °C and 300 °C was nearly 80%. During the rapid decomposition process, the chloride anion decomposed through dealkylation, whereas the cation simultaneously underwent alkyl migration and elimination (Liu et al., 2012).

3.2. Effect of AFEX pretreatment on Z. japonica

The structures of ZJ-AFEX were observed using an S-3700N scanning electron microscope (Hitachi, Ltd., Japan). Fig. 3 shows that the structures of *Z. japonica* were destroyed by AFEX pretreatment and the surfaces of the material became rougher after AFEX pretreatment. The pretreatment created greater pore volume in the small pore region in comparison with that of the untreated sample. A greater degree of structural damage accompanied an increase in the anhydrous ammonia-to-*Z. japonica* ratio. AFEX pretreatment of *Z. japonica* loosened the lignocellulosic matrix,

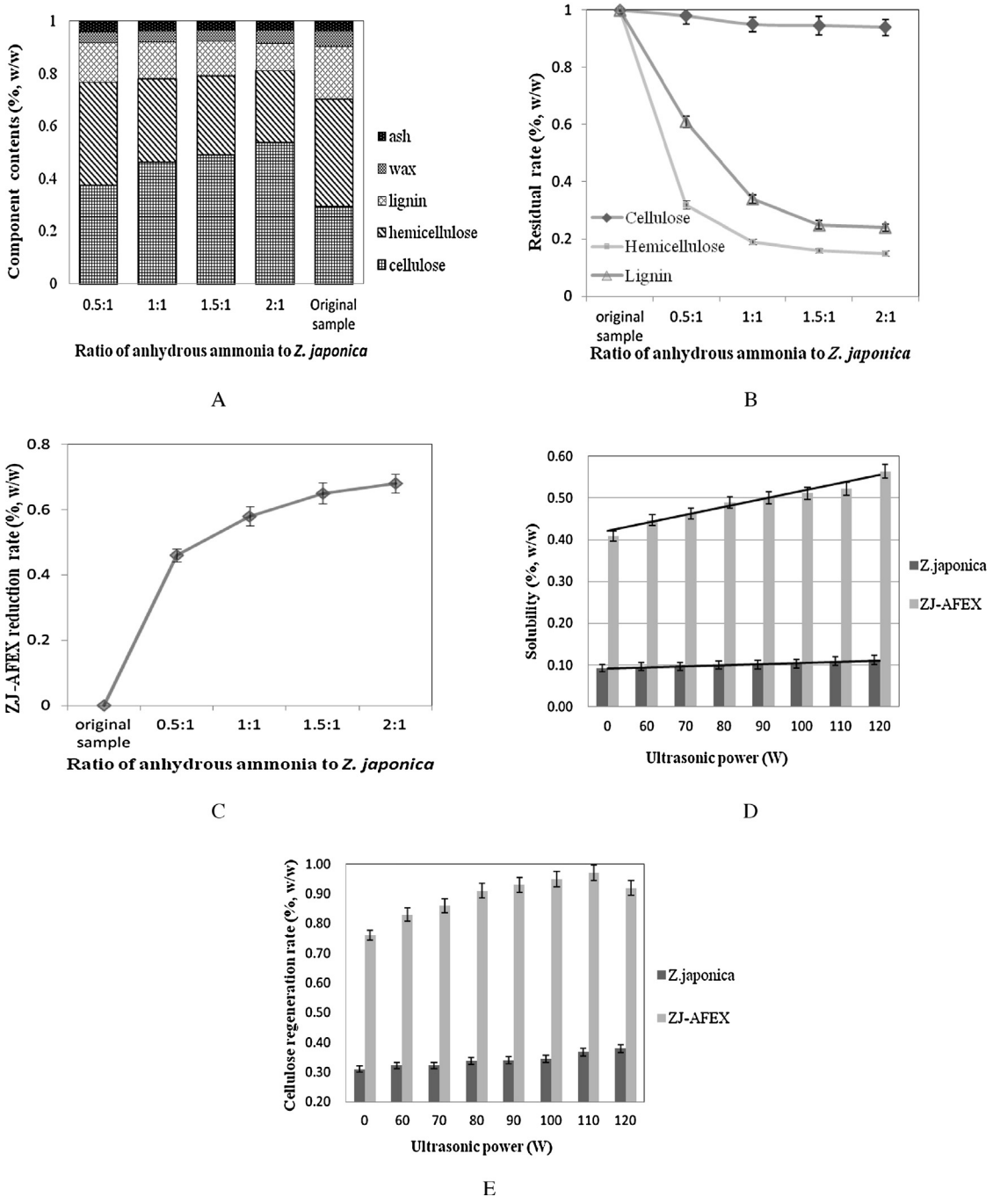

Fig. 4. The component contents of ZJ-AFEX samples (A), lignocellulose residual rate after AFEX pretreatment (B), mass loss of *Zoysia japonica* after AFEX pretreatment (C), *Zoysia japonica* and ZJ-AFEX samples dissolution in AMIMCl with ultrasonic vibration (D), and cellulose regeneration (E).

weakened intermolecular forces, and destroyed intramolecular and intermolecular hydrogen bonds, causing a more open three-dimensional organization of the cellulose, lignin, and hemicellulose polymers.

A comparison of the lignocellulosic content of ZJ-AFEX samples prepared using various ratios of anhydrous ammonia to *Z. japonica* is shown in Fig. 4A. The cellulose content of ZJ-AFEX samples increased relative to that of the original *Z. japonica* samples. However, the lignin and hemicellulose content decreased. The reduction became more obvious when the ratio of anhydrous ammonia to *Z. japonica* increased. Lignin provides a robust linkage between polysaccharide chains that hinders chemical accessibility to cellulose (Zhang & Lynd, 2004). As mentioned above, AFEX significantly reduced the lignin content. Furthermore, levels of wax and ash were somewhat reduced.

Fig. 4B and C show the lignocellulose residual rate and mass loss of *Z. japonica* after AFEX pretreatment, respectively. AFEX pretreatment reduced the mass of the *Z. japonica* sample significantly. However, hemicellulose and lignin accounted for most of the mass loss, and the cellulose mass was not substantially reduced. These results, combined with the analysis of the scanning electron microscopy results, demonstrate that AFEX pretreatment effectively disrupted the lignocellulose structure and increased the cellulose content. Hence, during the subsequent reaction, a larger amount of the cellulose component of ZJ-AFEX was in contact with the ionic liquid.

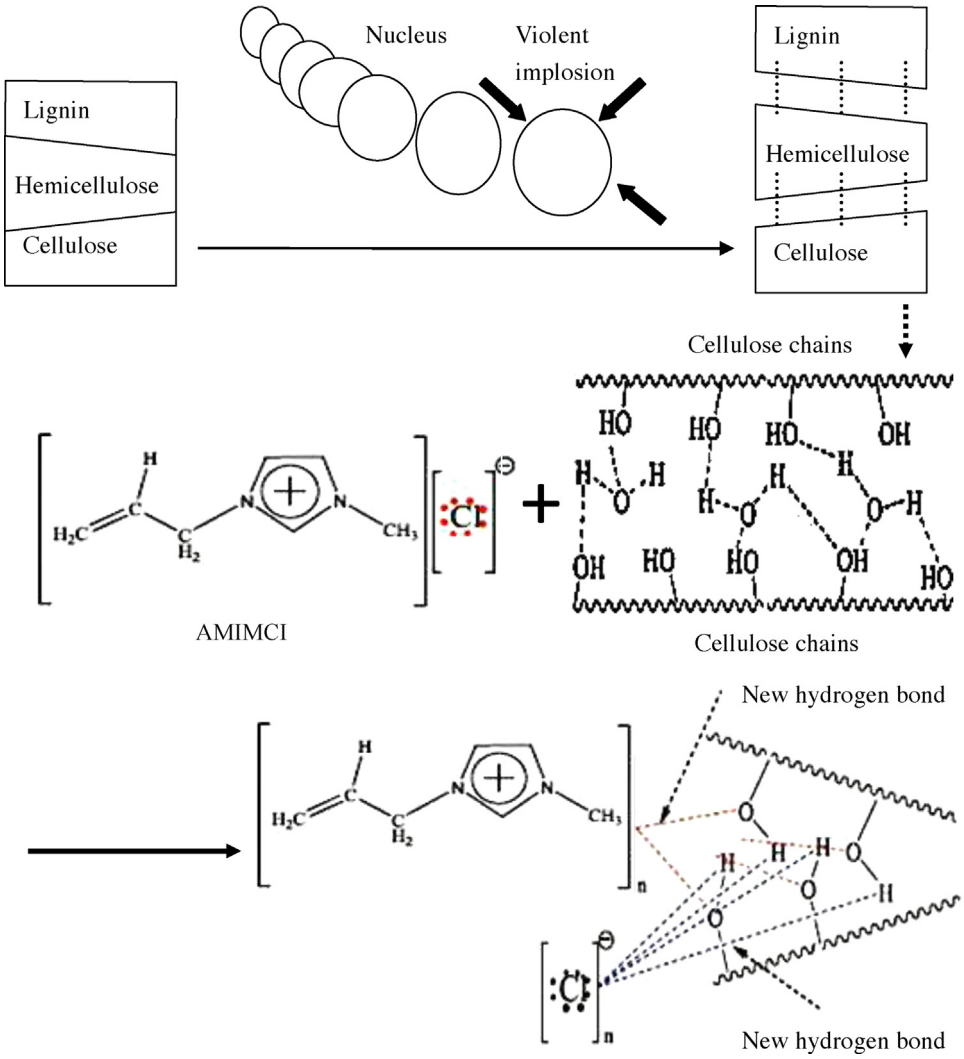

Fig. 5. Mechanism of the dissolution of cellulose in AMIMCl with ultrasonic vibration.

3.3. *Effect of ultrasound treatment on dissolution of cellulose in AMIMCl*

AMIMCl was used to dissolve the cellulose in *Z. japonica* and ZJ-AFEX samples. Fig. 4D shows the solubility of *Z. japonica* and ZJ-AFEX samples in AMIMCl (at 2:1 mass ratio of anhydrous ammonia to *Z. japonica* sample), which increased at higher ultrasonic power. However, the solubility of ZJ-AFEX sample presented a more obvious increasing trend. Ultrasonication improved the solubility because it facilitated the penetration and diffusion of AMIMCl in the entire structure of the samples. The lower solubility of *Z. japonica* confirms the enhancement of cellulose solubilization by AFEX pretreatment. The cellulose regeneration rate (Fig. 4E) increased at higher values of ultrasonic power within a certain range. The regeneration rate of the cellulose in ZJ-AFEX reached a peak of 97% when the ultrasonic power rose to 110 W. At higher power, it began to decline. The subsequent decrease may be due to intensified ultrasonic cavitation caused by excess ultrasonic energy, which initiates other reactions during dissolution and leads to cellulose degradation (Herfoster & Wintel, 1961).

Fig. 5 shows the mechanism of the dissolution of cellulose in AMIMCl with ultrasound treatment. The interaction between the ultrasonic vibrations and the medium leads to cavitation. The average distance between liquid molecules varies with molecular vibration according to the action of the pressure wave. When sufficient negative pressure is applied to the liquid, the distance between molecules exceeds the critical distance and cavitation bubbles appear (Aliyu & Hepher, 2000; Tang, Zhang, &, Chen, 2005). High local temperatures and compressed air are produced when the transient cavitation bubbles shrink or collapse, resulting in a powerful shock wave and jet stream (Vinatioru & Otilia, 1997). This promotes contact of the AMIMCl ionic liquid with the cells in the *Z. japonica* and ZJ-AFEX samples and the consequent disruption of the cells. The synthesized ionic liquid has special chemical structures, including a small chloride anion and a large 1-allyl-3-methylimidazolium cation (Lee, Doherty, Linhardt, & Dordick, 2009; Swatloski et al., 2002). Both anions and cations are considered to be involved in the dissolution process (Pinkert, Kenneth, Marsh,&, Mark, 2009). The oxygen and hydrogen atoms of the cellulose form electron donor–electron acceptor complexes with the charged species of the ionic liquids. The AMIMCl cations easily bind to oxygen in the intermolecular and intramolecular H-bonds between cellulose chains, whereas the chloride anions bind to the hydrogen atoms. This process breaks the intermolecular and intramolecular H-bonds of the cellulose chains, leading to the dissolution of the cellulose in the ionic liquid (Pinkert et al., 2009; Zhang et al., 2005).

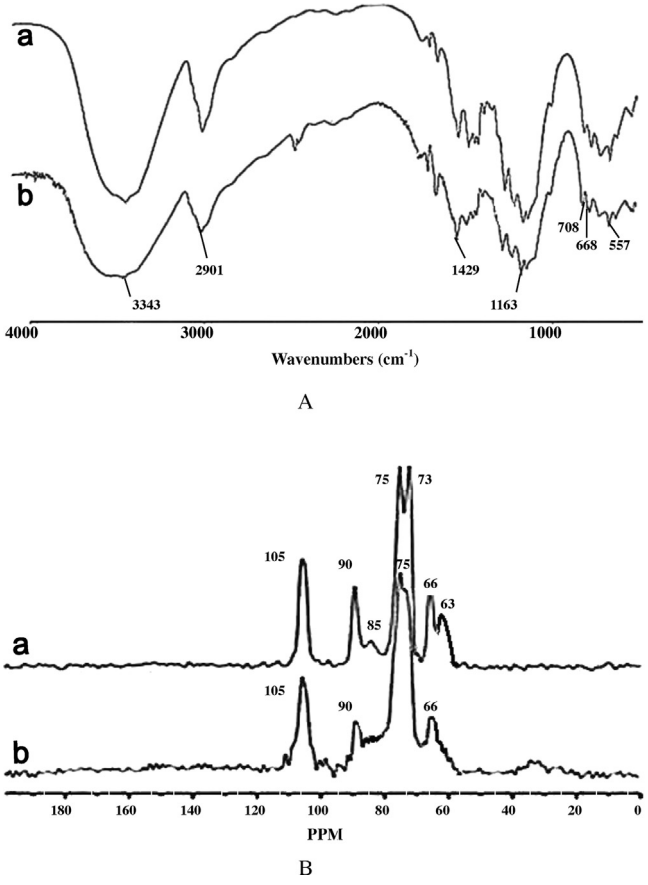

Fig. 6. FT-IR spectra (A) and ^{13}C NMR spectra (B) of microcrystalline cellulose (a) and regenerated cellulose (b).

3.4. Characterization of regenerated cellulose

To demonstrate that no other components were mixed with the regenerated cellulose, we used ^{13}C NMR and FTIR to compare microcrystalline cellulose (column chromatography grade; 99.99% purity) with regenerated cellulose from *Z. japonica*. As shown in Fig. 6A, the FTIR spectrum of regenerated cellulose is comparable to that of microcrystalline cellulose. The two spectra show similar absorbance peaks (positions listed in cm^{-1}): 3343 (—O—H stretching vibration), 2901 (C—H stretching vibration), 1429 (—CH_2 stretching vibration), and 1163 (C—O—C—O—C stretching vibration). Fig. 6B shows the ^{13}C NMR spectra of microcrystalline cellulose and regenerated cellulose. The microcrystalline cellulose has characteristic peaks at 105 (C1), 90 (C4, crystalline), 85 (C4, amorphous), 75 (C3/C5), 73 (C2), 66 (C6, crystalline), and 63 (C6, amorphous) ppm. The spectrum of regenerated cellulose also has characteristic peaks at 105, 90, 75, and 66 ppm, but peaks at 85, 73, and 63 ppm are not present. The reduced intensities of all the characteristic peaks of regenerated cellulose suggest that the crystallinity of the regenerated cellulose was lower (Wang, Li, Cao, & Tang, 2011). This point further proves that AMIMCl effectively dissolved the cellulose in *Z. japonica* through the disruption of intramolecular and intermolecular hydrogen bonds. In addition, multiple split peaks may be attributed to cellulose degradation products.

4. Conclusions

AMIMCl was synthesized and characterized through a series of test methods. AMIMCl exhibited high thermal stability and a considerable capacity to dissolve cellulose. AFEX pretreatment disrupted the lignocellulose structure and concomitantly increased the cellulose content of the *Z. japonica* sample. The ZJ-AFEX sample showed significant solubility in AMIMCl. Ultrasonication further improved the solubility of cellulose because it facilitated the penetration and diffusion of AMIMCl into the structure of the samples. The cellulose regeneration rate of ZJ-AFEX reached a maximum of 97% when the ultrasonic power was 110 W. The regenerated cellulose was similar to microcrystalline cellulose according to FTIR and NMR analyses.

Acknowledgments

We are grateful for financial support by the “Double Five” Science and Technology Project of the Colleges and Universities in Tianjin, China (SW20080004).

References

Aliyu, M., & Hepher, M. J. (2000). Effects of ultrasound energy on degradation of cellulose material. *Ultrasonics Sonochemistry*, *7*, 265–268.
Chundawat, S. P. S., Donohoe, B. S., da Costa Sousa, L., Elder, T., Agarwal, U. P., Lu, F., et al. (2011). Multi-scale visualization and characterization of lignocellulosic plant cell wall deconstruction during thermochemical pretreatment. *Energy & Environmental Science*, *4*, 973–984.
Chundawat, S. P., Vismeh, R., Sharma, L. N., Humpula, J. F., da Costa Sousa, L., Chambliss, C. K., et al. (2010). Multifaceted characterization of cell wall decomposition products formed during ammonia fiber expansion (AFEX) and dilute acid based pretreatments. *Bioresource Technology*, *101*, 8429–8438.
Deng, Y. C. (2003). Ionic liquids — the green material in the 21st century. *Chinese University Technology Transfer*, *10*, 33–35.
Doganand, H., & Hilmioglu, N. D. (2009). Dissolution of cellulose with NMMO by microwave heating. *Carbohydrate Polymers*, *75*(1), 90–94.
Heinze, T., & Liebert, T. (2001). Unconventional methods in cellulose functionalization. *Progress in Polymer Science*, *26*, 1689–1762.
Herfoster, L., & Wintel, H. M. (1961). *The Basic Principle and Application of Ultrasound*. Shanghai: Shanghai Science and Technology Press.
Kim, Y., Hendrickson, R., Mosier, N. S., Ladisch, M. R., Bals, B., Balan, V., et al. (2008). Enzyme hydrolysis and ethanol fermentation of liquid hot water and AFEX pretreated distillers' grains at high-solids loadings. *Bioresource Technology*, *99*, 5206–5215.
Klemm, D., Philipp, B., Heinze, T., Heinze, U., & Wagenknecht, W. (1998). *Comprehensive Cellulose Chemistry*. Weinheim: Wiley-VCH.
Lee, S. H., Doherty, T. V., Linhardt, R. J., & Dordick, J. S. (2009). Ionic liquid mediated selective extraction of lignin from wood leading to enhanced enzymatic cellulose hydrolysis. *Biotechnology and Bioengineering*, *102*(5), 1368–1376.
Li, C., Knierim, B., Manisseri, C., Arora, R., Scheller, H. V., Auer, M., et al. (2010). Comparison of dilute acid and ionic liquid pretreatment of switchgrass: biomass recalcitrance, delignification and enzymatic saccharification. *Bioresource Technology*, *101*, 4900–4906.
Liu, C. F., & Zhang, A. P. (2009). Dissolution of cellulose in novel green solvent ionic liquids and its application. *Progress in Chemistry*, *21*(9), 1800–1806.
Liu, D. T., Xia, K. F., Cai, W. H., Yang, R. D., Wang, L. Q., & Wang, B. (2012). Investigations about dissolution of cellulose in the 1-allyl-3-alkylimidazolium chloride ionic liquids. *Carbohydrate Polymers*, *87*, 1058–1064.
Mosier, N., Wyman, C., Dale, B., Elander, R., Lee, Y. Y., Holtzapple, M., et al. (2005). Features of promising technologies for pretreatment of lignocellulosic biomass. *Bioresource Technology*, *96*, 673–686.
Nattakan, S., Takashi, N., & Ton, P. (2009). All-cellulose composites of regenerated cellulose fibres by surface selective dissolution. *Composites: Part A*, *40*(4), 321–328.
Oh, S. Y., Yoo, D. I., Shin, Y., Kim, H. C., Kim, H. Y., & Chung, Y. S. (2005). Crystalline structure analysis of cellulose treated with sodium hydroxide and carbon dioxide by means of X-ray diffraction and FTIR spectroscopy. *Carbohydrate Research*, *340*(15), 2376–2391.
Pinkert, A., Kenneth, N., Marsh, S. P., & Mark, P. S. (2009). Ionic liquids and their interaction with cellulose. *Chemical Reviews*, *109*(12), 6712–6728.
Ren, Q., Wu, J., Zhang, J., He, J. S., & Guo, M. L. (2003). Synthesis of 1-allyl, 3-methylimidazolium-based room temperature ionic liquid and preliminary study of its dissolving cellulose. *Acta Polymerica Sinica*, *3*, 448–451.
Song, Y. B., Zhang, J., Gan, W. P., Zhou, J. P., & Zhang, L. N. (2010). Flocculation properties and antimicrobial activities of quaternized celluloses synthesized in NaOH/urea aqueous solution. *Industrial & Engineering Chemistry Research*, *49*(3), 1242–1246.
Swatloski, R. P., Spear, S. K., Holbrey, J. D., & Rogers, R. D. (2002). Dissolution of cellulose with ionic liquids. *Journal of the American Chemical Society*, *124*(18), 4974–4975.

Tang, A., Zhang, H., & Chen, G. (2005). Influence of ultrasound treatment on accessibility and regioselective oxidation reactivity of cellulose. *Ultrasonics Sonochemistry*, *12*, 467–472.

Vinatioru, M. T., & Otilia, R. (1997). The use of ultrasound for the extraction of bioactive principles from plant materials. *Ultrasonics Sonochemistry*, *4*, 135–136.

Wang, X. J., Li, H. Q., Cao, Y., & Tang, Q. (2011). Cellulose extraction from wood chip in an ionic liquid 1-allyl-3-methylimidazolium chloride (AmimCl). *Bioresource Technology*, *102*, 7959–7965.

Wu, J., Zhang, J., Zhang, H., He, J. S., Ren, Q., & Guo, M. L. (2004). Homogeneous acetylation of cellulose in a new ionic liquid. *Biomacromolecules*, *5*(2), 266–268.

Zhang, H., Wu, J., Zhang, J., & He, J. S. (2005). 1-Allyl-3-methylimidazolium chloride room temperature ionic liquid: a new and powerful nonderivatizing solvent for cellulose. *Macromolecules*, *38*(20), 8272–8277.

Zhang, J. M., Lv, Y. X., & Luo, N. (2011). Application research progress of ionic liquids in cellulose chemistry. *Polymer Bulletin*, *10*, 138–153.

Zhang, Y. H. P., & Lynd, L. R. (2004). Toward an aggregated understanding of enzymatic hydrolysis of cellulose: noncomplexed cellulase systems. *Biotechnology and Bioengineering*, *88*, 797–824.

Zhu, S. D., Wu, Y. X., Chen, Q. M., Yu, Z. N., Wang, C. W., Jin, S. W., et al. (2006). Dissolution of cellulose with ionic liquids and its application: a minireview. *Green Chemistry*, *8*, 325–327.